Spin-wave theory of the zero-point energy of solitons in one-dimensional magnets

1989 J. Phys.: Condens. Matter 1 6131

(http://iopscience.iop.org/0953-8984/1/35/012)

J. Phys.: Condens. Matter 1 (1989) 6131–6144. Printed in the UK

Spin-wave theory of the zero-point energy of solitons in one-dimensional magnets

D H Jones, Q A Pankhurst, M F Thomas and C E Johnson
Department of Physics, University of Liverpool, Liverpool L69 3BX, UK

Received 12 December 1988, in final form 13 March 1989

Abstract. It is known that quantum fluctuations significantly modify the energy required to produce a mobile domain wall, or soliton, on a chain of exchange-coupled magnetic atoms subject to an anisotropy field or magnetic field. We show here that spin-wave theory applied about the classical soliton solution to the sine–Gordon equation can be adapted to calculate these zero-point energy effects by matrix diagonalisation. The results for solitions on ferromagnetically coupled chains are qualitatively similar to those obtained by other techniques. In antiferromagnets, however, the quantum fluctuations appear to produce, under certain conditions, a negative soliton creation energy, i.e. a soliton-containing ground state. This situation is a result of the non-linear response of the zero-point energy to small changes in the effective anisotropy of the one-dimensional antiferromagnet.

1. Introduction

Quasi-one-dimensional magnets are of interest since they exhibit anomalously large magnetic fluctuations. While the small linear oscillations or spin waves, which provide a good description of the low-temperature properties, are well understood, the mathematical description of the non-linear mobile domain walls or solitons continues to arouse interest. The sine–Gordon equation

$$\partial^2\varphi/\partial z^2 - (1/c^2)(\partial^2\varphi/\partial t^2) = m^2 \sin\varphi, \tag{1}$$

which is obtained by making classical and continuum approximations to the magnetic Hamiltonian, provides a good starting point for the description of the non-linear excitations but the description of effects such as discreteness [1], soliton–soliton and soliton–magnon interactions [2–4], and coupling to the lattice [5] requires refinements to the basic theory.

Solitons (or at least non-linear fluctuations) have been observed by a variety of experimental techniques, including neutron scattering [6] and Mössbauer spectroscopy [7], via their effect on the spin-correlation function. They also contribute to the thermodynamics of the system [3]. The effect of solitons is particularly interesting when static magnetic fields are applied and it is possible to discuss the spin-flop phase transition in quasi-one-dimensional uniaxial antiferromagnets in terms of a soliton creation energy which is gradually reduced to zero by the applied field [8].

One of the most important refinements to the classical theory concerns the correction to the soliton creation energy produced by quantum fluctuations. These fluctuations

0953-8984/89/356131 + 14 $02.50

account qualitatively for the observed soliton energies in a variety of systems [9–11] which are systematically lower than those predicted from (1). The energy correction has been calculated using a variety of approximate techniques including semi-classical field theories [12–15], Bethe *ansatz* [16], Holstein–Primakoff formalism [17], variational methods [18] and numerical calculations [19]. Typically the agreement between theory and experiment is improved by these theories but is not perfect, especially for specific heat data [20, 21].

In this paper, we consider the application of a simple generalisation of spin-wave theory about the equilibrium configuration of spins on a stationary soliton to derive values for the quantum correction to the soliton creation energy. The spin-wave theory is flexible in that it can easily include experimentally relevant variations in the standard Hamiltonian, such as dipole–dipole interactions instead of single-ion anisotropy. The theory, which includes both in-plane and out-of-plane fluctuations, is expected to give a zero-point energy accurate to within a few per cent, even for $S = \frac{1}{2}$, since this is the error associated with the 1D antiferromagnet, which is the worst case for the spin-wave approximation. In general the results must be obtained numerically, by matrix diagonalisation, but this need not be considered a serious problem as numerical simulations have often played a significant role in soliton physics in the past [19, 21, 22]. In real materials, inter-chain interactions often play a crucial role and these could be modelled using the spin-wave technique, but to introduce the method we confine ourselves here to purely one-dimensional systems.

The starting point for much of the work on magnetic solitons is [23, 24]

$$E = \sum_j (-2J\boldsymbol{S}_j \cdot \boldsymbol{S}_{j+1} - K_1 S_{jz}^2 + K_2 S_{jy}^2 - g\beta \boldsymbol{B} \cdot \boldsymbol{S}_j) \tag{2}$$

which describes the classical energy of a spin system with $\boldsymbol{S}_j = (S_{jx}, S_{jy}, S_{jz})$, isotropic exchange coupling J, easy-axis anisotropy $K_1 > 0$, easy-plane anisotropy $K_2 > 0$ and magnetic field $\boldsymbol{B}$. K_2 tends to force the spins into the x–z plane and K_1 and $\boldsymbol{B}$ tend to have the effect of localising any twists of the spins within this plane. Where K_2 is sufficiently large for all the spins to lie in the x–z plane, the classical energy can be expressed, for a magnetic field along the z axis, as

$$E = S_c^2 \sum_j [-2J \cos(\theta_j - \theta_{j+1}) - K_1 \cos^2 \theta_j] - \sum_j g\beta B S_c \cos \theta_j \tag{3}$$

where θ_j is the angle between a given spin and the z axis, and the spins have classical length $S_c = [S(S+1)]^{1/2}$. The stable static configuration of spins subject to (1) can be found by setting $\mathrm{d}E/\mathrm{d}\theta_j = 0$:

$$2JS_c[\sin(\theta_j - \theta_{j+1}) + \sin(\theta_j - \theta_{j-1})] + K_1 S_c \sin(2\theta_j) + g\beta B \sin \theta_j = 0. \tag{4}$$

Application of the continuum approximation, in which the angles between adjacent spins become small gives, for $B = 0$,

$$\mathrm{d}^2\theta_j/\mathrm{d}j^2 = (m^2/2) \sin(2\theta_j) \tag{5}$$

where m^2 is K_1/J. This is essentially equation (1) without the time variable. A similar equation is obtained for $B \neq 0$, $K_1 = 0$. Although the soliton has interesting dynamics, this is not discussed below, i.e. we are concerned here only with the minimum energy required to create a soliton.

The solution with just one π twist is often of particular importance experimentally since all the spins are reversed after the soliton has passed, and so the spin correlation functions are strongly affected. This π soliton is a solution of (5) with

$$\theta(j) = 2\tan^{-1}[\exp(mj)]. \tag{6}$$

The energy is $E_S = 4S(S+1)(K_1J)^{1/2}$ and the width is about $(2J/K_1)^{1/2}$ spins. There is a mathematically similar 2π soliton for $B \neq 0$, $K_1 = 0$.

The soliton energy is sometimes expressed as $4S^2(K_1J)^{1/2}$ [8], where there is an implicit assumption that the soliton has zero-point energy $4S(K_1J)^{1/2}$ less than the untwisted magnetic chain. The situation is directly analogous to that for the simple ferromagnetic chain, for which the ground-state energy $-2JS^2$ per spin is obtained by addition of zero-point energy $2JS$ to the classical energy $-2JS(S+1)$ [25]. The remainder of this paper demonstrates that this implicit assumption is not always valid, especially for antiferromagnetic solitons.

2. Spin-wave theory of twisted chains

Although it has no immediate physical significance, the case of the closed chain (ring) with a number T of 2π twists distributed evenly over all chain links provides a good introduction to the application to solitons and some exact results can be obtained. This configuration is only stable if $\omega_A = 2K_1S = 0$, $\omega_B = g\beta B = 0$; we take $\hbar = 1$ throughout. It can be shown by derivation of the classical normal mode frequencies that the uniformly twisted chain requires $\omega_P > \omega_E(1 - \cos t)$ to be stable against fluctuations out of the x–z plane. Here $\omega_P = 2K_2S$, $\omega_E = 4JS$ and $t = t_j = \theta_j - \theta_{j+1} = 2\pi T/N$ is the twist per spin. A similar instability may occur in real solitions, particularly in applied fields, where the angle between adjacent spins can become large [26]. Transformation of (1) to a coordinate system in which each spin lies, at equilibrium, along its own local z axis [27] leads to a Hamiltonian with quadratic terms:

$$\begin{aligned}\mathcal{H}_j = -2J[&\cos^2 s_j(S_{j,y}S_{j+1,y} + S_{j,x}S_{j+1,x}) + \sin^2 s_j(S_{j,y}S_{j+1,y} - S_{j,x}S_{j+1,x}) \\ &+ \cos t_j\, S_{j,z}S_{j+1,z}] + K_2S_{j,y}^2\end{aligned} \tag{7}$$

where $s_j = t_j/2$, $\mathcal{H} = \Sigma_j\mathcal{H}_j$ and terms in $S_{j,x}S_{j+1,z} - S_{j,z}S_{j+1,x}$, which vanish at equilibrium, have been omitted. This can be expressed using the conventional spin deviation creation and annihilation operators defined by

$$S_{j,x} = (S/2)^{1/2}(a_j^\dagger + a_j) \qquad S_{j,y} = \mathrm{i}(S/2)^{1/2}(a_j^\dagger - a_j) \qquad S_{j,z} = S - a_j^\dagger a_j \tag{8}$$

as

$$\begin{aligned}\mathcal{H}_j = {} & c_1(a_j^\dagger a_j + \tfrac{1}{2}) + (c_2/2)(a_j^\dagger a_j^\dagger + a_j a_j) + (c_3/2)(a_j^\dagger a_{j+1} + a_j a_{j+1}^\dagger) \\ & + (c_4/2)(a_j^\dagger a_{j+1}^\dagger + a_j a_{j+1}) + c_5(a_{j+1}^\dagger a_{j+1} + \tfrac{1}{2}) \\ & + (c_6/2)(a_{j+1}^\dagger a_{j+1}^\dagger + a_{j+1}a_{j+1})\end{aligned} \tag{9}$$

where

$$\begin{aligned} &c_1 = (\omega_E\cos t + \omega_P)/2 && c_2 = -\omega_P/2 && c_3 = -\omega_E\cos^2 s \\ &c_4 = \omega_E\sin^2 s && c_5 = (\omega_E\cos t)/2 && c_6 = 0.\end{aligned} \tag{10}$$

Since the system has translational symmetry, it is appropriate to transform to momentum

space using $a_k^\dagger = \Sigma_j a_j^\dagger \exp(-ikr_j)$, where $-\pi/b < k < \pi/b$ and b is the lattice constant. This gives

$$\mathcal{H} = \sum_k \left((c_1 + \gamma_k c_3 + c_5) a_k^\dagger a_k + \frac{(c_2 + \gamma_k c_4 + c_6)(a_k^\dagger a_{-k}^\dagger + a_k a_{-k})}{2} \right) \tag{11}$$

where $\gamma_k = \cos k$. Now $[\mathcal{H}, \alpha_k^\dagger] = \omega_k \alpha_k^\dagger$, where $\alpha_k^\dagger = u_k a_k^\dagger + v_k a_{-k}$ is a creation operator for the coupled system. Equating terms in $a_k^\dagger$ and a_{-k} gives the frequencies as eigenvalues of the commutator matrix

$$\begin{pmatrix} c_1 + \gamma_k c_3 + c_5 & -c_2 - \gamma_k c_4 - c_6 \\ c_2 + \gamma_k c_4 + c_6 & -c_1 - \gamma_k c_3 - c_5 \end{pmatrix}. \tag{12}$$

Therefore

$$\omega_k^2 = \omega_E \cos t(1 - \gamma_k)[\omega_E(\cos t - \gamma_k) + \omega_P]. \tag{13}$$

It can be seen that the correct dispersion relations for the ferromagnet ($\omega_E > 0$) and antiferromagnet ($\omega_E < 0$) with zero anisotropy are obtained by putting $\omega_P = 0$ with $t = 0$ and $t = \pi$, respectively.

To a first approximation the requirement that $\omega_k^2 > 0$ reproduces the stability condition $\omega_P > \omega_E(1 - \cos t)$. However, since γ_k can take only discrete values corresponding to $k = 2\pi l/N$, $l = 1, \ldots, N$, the exact result is more complicated. Thus for $\omega_E > 0$ the chain with $\omega_P = 0$ is just stable for $t = 2\pi/N$, i.e. for a single 2π twist, since the ω_P-containing term of (13) becomes negative only where $1 - \gamma_k = 0$. The antiferromagnet is different since the instability associated with out-of-plane displacements appears at $k = \pi$, $\gamma_k = -1$. Here there is no other term in the product (13) which vanishes; hence, if $\omega_P = 0$, the twisted chain is unstable for any $T \neq 0$.

The zero-point energy of the twisted chain can be calculated by summing $\omega_k/2$ in the standard way. In general, this will be different from the zero-point energy of the untwisted chain by an amount which is the quantum correction to the twist creation energy.

In the limit of large N, (13) can be integrated (as long as $\omega_k^2 > 0$). The zero-point energy becomes

$$E_Q = |\omega_E||\cos t|^{1/2} \frac{1}{2\pi} \int_0^\pi (1 - \cos k)^{1/2} \left(|\cos t| \mp \cos k + \frac{\omega_P}{|\omega_E|} \right)^{1/2} \mathrm{d}k \tag{14}$$

i.e. $E_Q \simeq \omega_E(1 - t^2/4)I$, where

$$I = \frac{1}{2\pi} \int_0^\pi (1 - \cos k)^{1/2} (1 \mp \cos k + 2\omega'_P)^{1/2} \, \mathrm{d}k \tag{15}$$

and $2\omega'_P = \omega_P/|\omega_E| - t^2/2$. It can be seen that a small twist angle t affects E_Q in two ways: by scaling the entire dispersion curve by $1 - t^2/4$ and by reducing the effective easy-plane anisotropy. For $\omega_E > 0$, I reduces to

$$I_{FM} = \frac{2}{\pi}(1 + \omega'_P) \int_0^{(1+\omega'_P)^{-1/2}} (1 - x^2)^{1/2} \, \mathrm{d}x \tag{16}$$

while, for $\omega_E < 0$,

$$I_{AM} = \frac{2}{\pi} \omega'_P \int_0^{\omega'^{-1/2}_P} (1 + x^2)^{1/2} \, \mathrm{d}x. \tag{17}$$

Both are standard integrals.

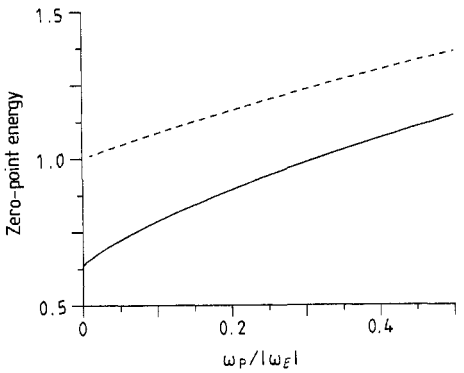

Figure 1. Zero-point energies per spin, in units of $\omega_E/2$ for magnetic chains as a function of easy-plane anisotropy $\omega_P/|\omega_E|$: ——, $\omega_E < 0$; ---, $\omega_E > 0$.

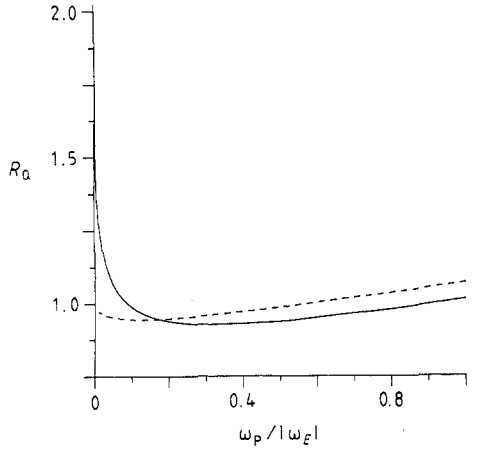

Figure 2. R_Q, the ratio of the exact zero-point energy to that required to produce a twist creation energy proportional to S^2, as a function of easy-plane anisotropy for $\omega_E < 0$ (——) and $\omega_E > 0$ (---).

In considering the quantum correction to the twist energy E_t, it is convenient to define R_Q by

$$E_t = E_0[S(S+1) - R_Q S] \tag{18}$$

where $E_0 S(S+1) = E_{cl}$, the classical twist creation energy. R_Q is therefore the ratio of the quantum correction to the twist energy to that quantum correction which would be required to give a twist energy proportional to S^2. If $R_Q > S+1$, then the total twist creation is negative, i.e. the ground state of the system will contain twists. There will be an energy barrier to twist formation since both the twisted and the untwisted states are stable, but we do not discuss the kinetics of the twisting process.

For small t the classical twist creation energy per atom is, from (3),

$$E_{cl} = \omega_E(S+1)t^2/4. \tag{19}$$

Therefore

$$R_Q = -(4/\omega_E t^2)[E_Q(t) - E_Q(0)] \simeq -(4/\omega_E t^2)t^2 \, \mathrm{d}E_Q/d(t^2) \tag{20}$$

but $E_Q = \omega_E(1 - t^2/4)I$; differentiating this gives

$$R_Q = I + \mathrm{d}I/\mathrm{d}\omega_P'. \tag{21}$$

Application of this result to (16) and (17) gives

$$R_Q(\omega_E > 0) = (1/\pi)\{x^{-2}[x(1-x^2)^{1/2} + \sin^{-1} x] + \sin^{-1} x\} \tag{22}$$

where $x = (1 + \omega_P')^{-1/2}$ and

$$R_Q(\omega_E < 0) = (1/\pi)\{y^{-2}[y(1+y^2)^{1/2} + \sinh^{-1} y] + \sinh^{-1} y\} \tag{23}$$

where $y = \omega_P'^{-1/2}$. As is often found in spin-wave theory, the trigonometric functions found for $\omega_E > 0$ are replaced by hyperbolic functions for $\omega_E < 0$. The zero-point energies for typical values of ω_P and t, for both signs of ω_E are shown in figure 1. The derived R_Q for the creation of a single twist are shown in figure 2.

It can be seen that R_Q diverges for large ω_P since for $\omega_P \gg \omega_E$ the dispersion relation reduces to

$$\omega_k = (2\omega_E \omega_P \cos t)^{1/2} \sin(k/2). \tag{24}$$

The quantum correction becomes greater than the classical energy for

$$\omega_P/\omega_E \geqslant \pi^2(S+1)^2/2. \tag{25}$$

For the ferromagnet, $R_Q \rightarrow 1$ as $\omega_P \rightarrow 0$. For the antiferromagnet the situation is quite different, the low ω_P' expansion of R_Q is

$$R_Q(\omega_P' \rightarrow 0) = (\ln 2)/\pi - (\ln \omega_P')/2\pi. \tag{26}$$

This result means that the antiferromagnetic ring may become unstable with respect to twist formation for certain critical ring sizes which allow twists to be stable, for small ω_P. The critical ring sizes are about 60 for $S = \frac{1}{2}$, about 300 for $S = 1$ and increase by a factor of about 5 for each further half-spin.

Strictly speaking the $S = \frac{1}{2}$ result cannot be correct since single-ion anisotropy cannot affect spins $S = \frac{1}{2}$. However, the only effect of replacing single-ion anisotropy by an exchange anisotropy $S_{iz}S_{i+1,z}$ of a sign which also creates an easy plane is to multiply ω_P by γ_k in expressions such as (13). This only slightly modifies the rest of the derivation, which remains qualitatively correct for all ω_P and exactly correct in the low-ω_P limit. Exchange anisotropy is possible for all values of S.

It can be seen from figure 1 that, if the energy is decreased by the formation of a single twist, then it is likely that the antiferromagnetic chain will lose even more energy by gaining second and subsequent twists since the gradient of the zero-point energy is increased as the effective anisotropy is decreased. It seems reasonable to suppose that the twisting process, once started, will continue until ω_P is exactly balanced by twists, i.e. $\omega_P' = 0$. This gives the following picture of the ground state of the antiferromagnetic ring as ω_P is reduced from a large value, say $\omega_P = \omega_E$. Initially $R_Q \simeq 1$ and so the twist creation energy is positive. As ω_P is reduced, a critical value, $R_Q > S + 1$, is reached at which the system loses more quantum fluctuation energy than it gains classical energy by twisting to $\omega_P' = 0$. This critical ω_P represents the most twisted state since, as ω_P is further reduced, the t^2 necessary to produce $\omega_P' = 0$ is decreased and the chain gradually unravels, becoming untwisted again at $\omega_P = 0$.

In summary, an isotropically coupled ring of spins becomes unstable with respect to twisting for large planar anisotropy whatever the sign of ω_E. Only the antiferromagnetic ring becomes unstable for small ω_P. The peculiar behaviour of the antiferromagnet is a consequence of the non-linear behaviour of the dispersion curve near to $k = \pi$. We show below that similar instability at a low anisotropy may occur in antiferromagnetic soliton systems. This may have observable consequences for real materials.

3. Application to solitons

The application to solitons follows the same lines as above except that, since there is now no translational symmetry, the commutator matrix must be solved numerically in real space and it is not possible to obtain closed-form expressions for the soliton creation energy. Although it would be possible to use the continuum expression (6), the effects of discreteness can easily be included in the calculation. Thus, equation (4) allows θ_{j-2} to be calculated given θ_j and θ_{j-1} and this remains true as long as the Hamiltonian is

restricted to nearest-neighbour interactions. Hence, if the angle between two adjacent spins is chosen, the angles of all other spins can be calculated. The angle can then be varied until the energy of the system is at a local minimum. In the study of solitons it is convenient to choose two atoms at the centre of a finite length of chain such that their average angle with respect to the applied field or easy axis is half the total twist angle of the required soliton. Thus for a π soliton in a ferromagnetic chain the central atoms are chosen to straddle the angle $\theta = \pi/2$. It is not necessary to apply constraints to the end atoms.

There are always questions concerning the validity of spin-wave theories in finite systems but we have shown that the finite-chain spin-wave theory can be applied with some success to the spin reduction in doped quasi-one-dimensional magnets [28] and this gives us increased confidence here. The zero-point energy is also likely to be more accurate than the zero-point spin reduction, which diverges in one dimension when the anisotropy vanishes. It is notable that spin-wave theory gives exactly correct values for the zero-point energy of the two- and four-membered antiferromagnetic rings, even for $S = \frac{1}{2}$.

It is essential that boundary effects are eliminated from the calculations of the changes due to the presence of the soliton, by taking chains of length much larger than the soliton width. In practice this is not usually a severe constraint since zero-point energies obtained by spin-wave theory are, at worst, in the antiferromagnet accurate to only about 2% and it is easy to make boundary effects insignificant at this level.

The commutator matrix for the soliton problem is obtained by considering the commutator of $\mathcal{H}$ with the creation and annihilation operators at each of the N sites. Thus,

$$[\mathcal{H}, a_j^\dagger] = (c_{3,j-1}/2)a_{j-1}^\dagger + (c_{4,j-1}/2)a_{j-1} + (c_{1,j} + c_{5,j-1})a_j^\dagger + (c_{2,j} + c_{6,j-1})a_j + (c_{3,j}/2)a_{j+1}^\dagger + (c_{4,j}/2)a_{j+1}. \tag{27}$$

Two subscripts are now necessary on the coefficients c since θ_j and hence t_j and $s_j = t_j/2$ depend on j. The uniaxial anisotropy and applied field modifies the coefficients given in (10) to produce

$$\begin{aligned} c_{1j} &= [\omega_E \cos t_j + \omega_A(3\cos^2\theta_j - 1) + \omega_P]/2 + \omega_B \cos\theta_j \qquad c_{4j} = \omega_E \sin^2 s_j \\ c_{2j} &= -(\omega_A \sin^2\theta_j + \omega_P)/2 \qquad\qquad c_{5j} = (\omega_E \cos t_j)/2 \\ c_{3j} &= -\omega_E \cos^2 s_j \qquad\qquad c_{6j} = 0 \end{aligned} \tag{28}$$

where $\omega_B = g\beta B$ and we consider here only fields along the z axis. Writing $[\mathcal{H}, \alpha^\dagger] = \omega\alpha^\dagger$, where $\alpha^\dagger = u_1 a_1^\dagger + u_2 a_1 + u_3 a_2^\dagger + \ldots$ and equating terms in $a_1^\dagger, a_1, \ldots$ gives a matrix in which each row contains six non-zero elements placed around the leading diagonal. Thus the rows which arise from $a_j^\dagger$ and a_j are

$$\begin{pmatrix} \ldots & \ldots & \ldots & \ldots & \ldots & \ldots & \ldots & \ldots & \ldots & \ldots \\ \ldots & 0 & c_{3,j-1}/2 & -c_{4,j-1}/2 & d_j & -c_{2,j} & c_{3,j}/2 & -c_{4,j}/2 & 0 & \ldots \\ \ldots & 0 & c_{4,j-1}/2 & -c_{3,j-1}/2 & c_{2,j} & -d_j & c_{4,j}/2 & -c_{3,j}/2 & 0 & \ldots \\ \ldots & \ldots & \ldots & \ldots & \ldots & \ldots & \ldots & \ldots & \ldots & \ldots \end{pmatrix} \tag{29}$$

where $d_j = c_{1,j} + c_{5,j-1}$ is the diagonal element. The eigenvalues of the matrix occur in pairs related by a change in sign, which correspond to creation and annihilation operators

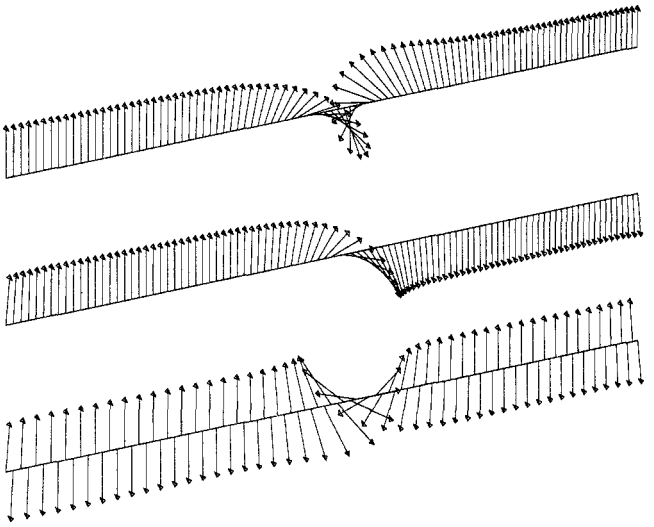

Figure 3. Representations of 2π ferromagnetic, π ferromagnetic and π antiferromagnetic solitons used in the numerical calculations. All the spins lie in the plane perpendicular to the chain axis.

for the coupled system. As usual the zero-point energy is half the sum of the positive eigenvalues.

4. Results

The above method has been applied to three simple soliton systems: the 2π soliton in an easy-plane ferromagnet, the '2π ferromagnetic' soliton, which has a finite length only in applied field; the π soliton of the planar ferromagnet with easy-axis anisotropy, the 'π ferromagnetic' soliton, which is stable only in zero applied field; and the π soliton in the easy-axis antiferromagnet, the 'π antiferromagnetic' soliton, which is considered here only in zero applied field. Although the case of the easy-axis antiferromagnet in applied field is particularly interesting, especially in the region of the spin-flop transition, this particular system is dominated by intra-chain effects which cause soliton pairing [29] and will be considered separately in a later work.

Some typical solitons used in the calculations, generated by the numerical method described above, are drawn in figure 3.

To obtain a good understanding of the changes associated with soliton formation, it is useful to consider the changes in the eigenvalues and eigenvectors of matrix (29) as a function of wavevector k rather than simply discussing integrated quantities such as R_Q. Even where a soliton is present, k can be defined in terms of the asymptotic behaviour of the spin wave far away from the soliton by making k the subject of the dispersion relation for the unperturbed chain, $k = k(\omega)$. The construction of our matrix problem results in a one-to-one correspondence between the eigenvalues of the chains with and without solitons. Each excitation with energy greater than that of the lowest frequency of the unperturbed chain, $\omega > \omega_0 = \omega(k = 0)$, can be associated through k with a wavelength λ, and the change in λ on soliton formation can be used to define a 'phase shift' due to the soliton. Phase shifts have played an important role in the theory of

solitons [15, 30] since they can be related to the correlation functions and hence to thermodynamic properties.

The free ends of magnetic chains are associated with particular values for the phase, but these are relatively easy to include in the calculation. Thus for a ferromagnetic chain with $\omega_P \ll \omega_E$ the excitations take the form of (real) standing waves with coefficients $\sin(kx + \varphi)$, where x is the position along the chain and φ represents the phase. For a chain with atoms lying at $x = 1, \ldots, x = N$, φ is determined by the condition that there are anti-nodes at $x = \frac{1}{2}$ and $x = N + \frac{1}{2}$. For the antiferromagnet the end effects are more complicated but, for $\omega_P = 0$, they can be eliminated from the calculations on chains with even numbers of atoms since the phase shifts at the two ends cancel. This leads to wavelengths for the excitations of the chains without solitons which are simple fractions of N in both antiferromagnets and ferromagnets. The expression for the phase shift δ is

$$M\lambda/2 = N + \delta\lambda/2\pi \qquad \text{i.e. } \delta = \pi M - kN \tag{30}$$

where M is the number of nodes in the eigenvector. Typically the phase shifts are different for even and odd modes, denoted δ^+ and δ^-.

Bound states, with $\omega < \omega_0$, decay exponentially and cannot be associated with a phase shift. The number of bound states associated with soliton formation depends on the type of soliton but there is always one bound state with an energy which is very small and tends to zero as the chain length increases. This mode corresponds to propagation of the soliton along the chain, a zero-energy process in the absence of discreteness and end effects.

The antiferromagnetic chain with uniaxial anisotropy has two extra bound states, independent of the existence of a soliton, which are associated with the chain ends and decay exponentially into the chain. Analysis of the form of the matrix at chain ends shows that these states have energy given by $\omega^2 \simeq \omega_A(\omega_E + \omega_A)$ compared with $\omega_0^2 = \omega_A(2\omega_E + \omega_A)$.

4.1. The 2π ferromagnetic soliton

Quantum effects in the 2π ferromagnetic soliton system have been analysed in some detail using a semi-classical continuum approximation [15] and it is possible to compare those results with the results obtained by the present method. For the 2π ferromagnetic soliton there is a second bound state at an energy $\omega \simeq \omega_0(1 - 8\omega_B^2/9\omega_P^2)$. Our calculations qualitatively reproduce the results, but it is not possible to test, for instance, the factor $\frac{8}{9}$ since the bound-state energy converges rather slowly with increasing chain length. This is the only example in our calculations for which the finite chain length is a limitation. The bound-state energy is never less than about $0.9\omega_0$ as this soliton becomes unstable for $\omega_P/\omega_B < 3$. This feature is reproduced well in our calculations.

Phase shifts for chains with $\omega_P/\omega_B = 5$ are plotted as a function of $q = k(\omega_E/2\omega_B)^{1/2}$ in figure 4 which may be directly compared with figure 1 of [30]. The close similarity of the figures is good evidence of the reliability of our calculations. A plot of the phase shift over the whole of the interval $0 < k < \pi$ shows that the shift does not decay to zero for large q but drops to a minimum proportional to $\omega_B^{1/2}/\omega_E$ near to $k = \pi/2$. There is a second maximum in the phase shift near to $k = \pi$; this feature is shown in figure 5 for two applied fields. It can be seen that the region over which the odd- and even-mode phase shifts are split decreases in size as the field decreases, i.e. as the soliton gets larger. It is perhaps simpler to present the information of figure 5 as a plot of the difference in energy of the normal modes produced on soliton formation; this is done in figure 6. The

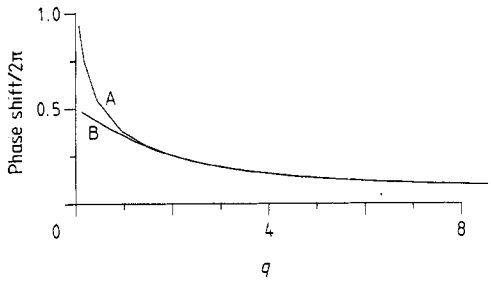

Figure 4. Phase shift $\delta(q)$ for a magnon of wavevector q in the presence of a static 2π ferromagnetic soliton for $\omega_P/\omega_B = 5$ (curve A, δ^+; curve B, δ^-).

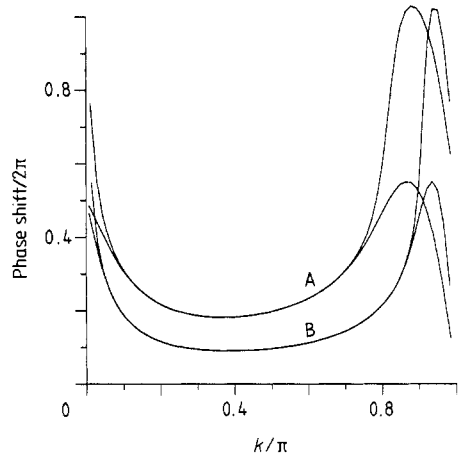

Figure 5. Phase shifts $\delta(k)$ for 2π ferromagnetic solitons with $\omega_P/\omega_B = 5$: curve A, $\omega_B = 0.02\omega_E$; curve B, $\omega_B = 0.005\omega_E$.

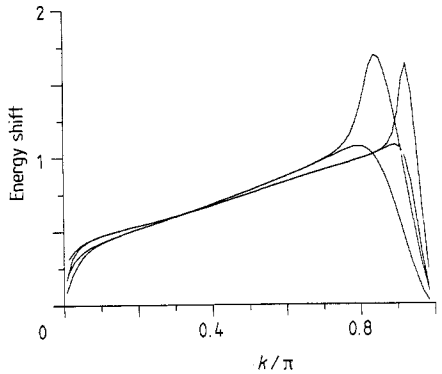

Figure 6. Energy shifts $\Delta E(k)$ for the solitons in figure 5. The energy differences are normalised to the average value which woud be required to produce $R_Q = 1$.

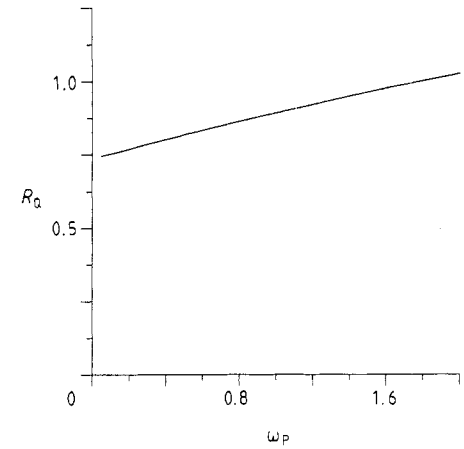

Figure 7. R_Q as a function of easy-plane anisotropy for the 2π ferromagnetic soliton for an applied field $\omega_B = 0.005\omega_E$.

energy difference has been divided by the average energy per mode which would be required to produce $R_Q = 1$, to make the results independent of chain length. R_Q is the average of the energy difference curve.

It can be seen that the energy difference curve is nearly a straight line through a point $k = \pi/2$, $\Delta E \simeq 0.75$, except in the regions for which the even and odd modes are split.

The variation is R_Q with ω_P at constant ω_B for the 2π ferromagnetic soliton, is shown in figure 7. R_Q tends to about 0.75 as ω_P, $\omega_B \rightarrow 0$ and is only weakly dependent on small ω_P. This value is different from that found in [15] since there the soliton energy is expressed as $E_S \propto [S_c - \frac{1}{2} + O(1/S_c)](S + 1)$, i.e. $R_Q = S_c - \frac{1}{2} + O(1/S_c) - S = 1 + O(1/S_c) = 1$ to order 1. We believe that our result is more accurate since it includes the

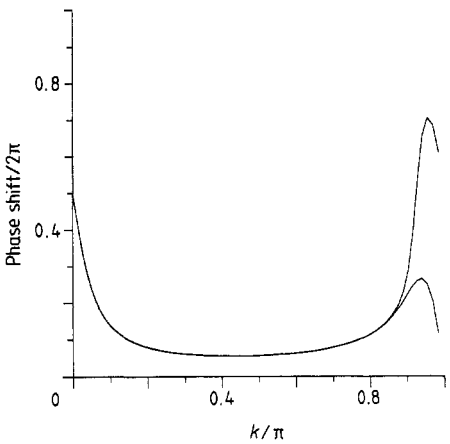

Figure 8. Phase shifts $\delta(k)$ for a π ferromagnetic soliton with $\omega_A = 0.01\omega_E$, $\omega_P = 0$.

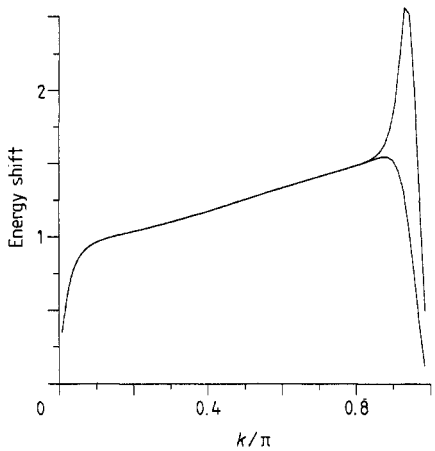

Figure 9. Energy shifts, as in figure 6, for the π ferromagnetic soliton in figure 8.

influence of the discrete lattice, and also because spin-wave theory is intrinsically rather accurate when used to estimate first-order quantities such as R_Q. For increasing ω_P the behaviour is qualitatively similar to that of the twisted ferromagnetic chain.

4.2. The π ferromagnetic soliton

The π ferromagnetic soliton is stable for all values of ω_P. There is only one true bound state, with $\omega = 0$, but a mode with $k = 0$ (i.e. a 'nearly' bound state) and a phase shift of exactly π remains after soliton formation. The phase shifts for the other modes, both even and odd, tend to π as $k \to 0$.

Phase shifts and energy differences are plotted as a function of k in figure 8 and figure 9 respectively. The energy difference curve is shifted systematically upwards compared with that of the 2π ferromagnetic soliton, which gives rise to a larger R_Q ($\simeq 1.25$) for small ω_P. $R_Q(\omega_P)$ is plotted for the π ferromagnetic solition and the π antiferromagnetic soliton, which both have classical energy $4S_c^2(JK)^{1/2}$, in figure 10. R_Q for the π ferromagnetic soliton rises continuously, becoming greater than 1.5 for $\omega_P > 0.3\omega_E$. Beyond this point the $S = \frac{1}{2}$ system would therefore become unstable with respect to soliton formation.

4.3. The π antiferromagnetic soliton

The π antiferromagnetic soliton in zero field exhibits the most complicated behaviour. It is necessary to take rather long chains so that the bound states associated with the chain ends are unaffected by soliton formation. For $\omega_P = 0$ there are two soliton bound states, each with $\omega = 0$. The energy of the mode which is not a propagation mode increases as $(2\omega_P\omega_E)^{1/2}$. This bound-state energy always lies below the energy for $k = \pi$ but it may lie above the energy of unbound states with $k \simeq 0$, for which $\omega^2 = \omega_A(2\omega_E + \omega_A + \omega_P)$. Thus the bound state associated with the soliton can have an energy greater than some of the unbound states.

The phase shifts and R_Q-values are strongly dependent on both ω_A and ω_P where these quantities are both small. Thus, figure 10 is drawn for a particular value $\omega_A =$

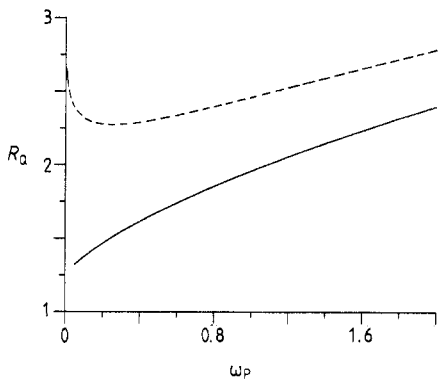

Figure 10. R_Q as a function of easy-plane anisotropy for the π soliton on a ferromagnetic chain (——) and an antiferromagnetic chain (– – –) with easy-axis anisotropy $\omega_A = 0.01\omega_E$.

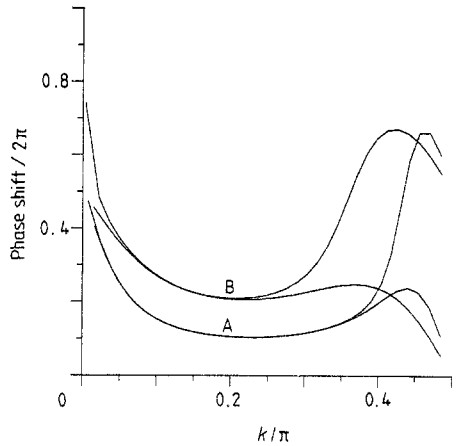

Figure 11. Phase shifts for π antiferromagnetic solitons with $\omega_A = 0.01\omega_E$ (curves A) and $\omega_A = 0.04\omega_E$ (curves B).

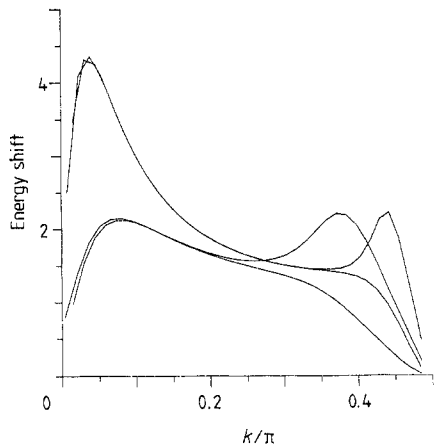

Figure 12. Energy shifts, as in figure 6, for the π antiferromagnetic soliton in figure 11.

$0.04\omega_E$. In general, discussion for $\omega_P > 0$ is complicated because the dispersion curve is no longer symmetric about $\pi/2$ and because of rather complicated end effects. We therefore confine our discussion to $\omega_P = 0$.

Plots of phase shifts and energy differences for $\omega_P = 0$ are shown in figure 11 and figure 12 for two values of ω_A. It can be seen that the phase shifts for this soliton are not strikingly different from those discussed previously, but the qualitatively different nature of the dispersion curve leads to much larger energy shifts. R_Q (plotted in figure 10) increases, probably logarithmically as ω_A decreases. We find, for instance, that $R_Q > 3.5$ for $\omega_A/\omega_E \simeq 0.002$, this value being relevant to the $S = \frac{5}{2}$ chain. We therfore conclude that the antiferromagnetic chain with less than a critical amount of uniaxial anisotropy will be unstable to soliton formation unless there is a stabilising planar anisotropy field. This result is qualitatively identical with that found for the twisted antiferromagnetic chain.

In contradiction to the above conclusion, real antiferromagnets with small uniaxial anisotropy are known. We believe that the most likely resolution of this difficulty is that quantum fluctuations are suppressed by inter-chain interactions in two ways. Most simply the high R_Q is due to non-linear response of the dispersion curve to small changes in effective anisotropy near to $k = \pi$. As the dimensionality increases, the importance of such extreme k is reduced. Interactions between antiferromagnetic chains will also produce a staggered field, which causes pairing of π solitons. The quantum fluctuations of the paired system may be different from those of the single soliton.

In general terms the conclusion that the soliton creation energy must be strongly dependent on inter-chain interactions is not surprising since it is these interactions which cause the magnetic ordering which would otherwise be destroyed by fluctuations. The divergence of R_Q may in this sense be compared with the similar logarithimic divergence of the spin reduction as $\omega_P \rightarrow 0$. The spin reduction is known to be sharply reduced by even weak three-dimensional interactions.

5. Conclusions

We have shown that spin-wave theory is a versatile method for calculating the static properties of solitons on magnetic chains. Our results for the 2π ferromagnetic soliton are similar to those obtained by other methods except that we find a smaller reduction in the soliton creation energy since R_Q is 0.75 and not 1.0. For the π ferromagnetic soliton in zero applied field the energy shifts become larger so that the soliton energy is reduced below $S(2\omega_E\omega_A)^{1/2}$. This soliton has only one true bound state. Small amounts of planar anisotropy (which are necessary for the stability of the 2π ferromagnetic soliton) have only a small effect on the energy of the ferromagnetic solitons.

For $\omega_P = 0$ the π antiferromagnetic soliton has negative creation energy if ω_A/ω_E is smaller than a critical value which depends on the spin. Although inter-chain interactions may modify this result in real systems, we believe that it may have important consequences where the anisotropy or effective anisotropy is small. This may occur, for example, near to the spin-flop phase transition. The soliton creation energy is very strongly dependent on small amounts of planar anisotropy. It will be necessary to include interactions between chains in the theory before the quantitative results can be applied to experimental systems.

The application of spin-wave theory here is new in that it introduces the idea that quantum fluctuations may change the nature of the ground state. In conventional applications of spin-wave theory it can be assumed that the minima of the zero-point energy and the classical energy occur at the same point, the quantum fluctuations in this sense reinforcing the classical configuration. In some of the applications discussed above, there is a conflict between the classical stability, which requires simply that $\omega_k(k = 0) \geqslant 0$, and the quantum fluctuations which involve the whole of the dispersion curve. The ground state is the result of a compromise between the two effects, the quantum contribution having weight $1/S$. We would expect conflicts between the classical and quantum contributions to the energy to occur whenever the zero-point energy contains a term which is logarithmic in small amounts of added anisotropy, as in the uniaxial antiferromagnet.

References

[1] Liebmann R, Benke G and Schobinger M 1987 *J. Phys. C: Solid State Phys.* **20** 3719

[2] Allroth E and Mikeska H J 1980 *J. Phys. C: Solid State Phys.* **13** L725
[3] Currie J F, Krumhansi J A, Bishop A R and Trullinger S E 1980 *Phys. Rev.* B **22** 477
[4] Ravelo R, El-Batanouny E, Willis C R and Sodano P 1988 *Phys. Rev.* B **38** 4817
[5] Cieplak M and Tursi L A 1980 *J. Phys. C: Solid State Phys.* **13** L777
[6] Kjems J and Steiner M 1978 *Phys. Rev. Lett.* **41** 1137
[7] de Groot H J M, de Jongh L J, El Massalami M, Smit H H A and Thiel R C 1986 *Hyperfine Interact.* **27** 93
[8] de Jongh L J and de Groot H J M 1985 *Solid State Commun.* **53** 731
[9] Pini M G and Rettori A 1984 *Phys. Rev.* B **29** 5246
[10] Tinus A M C, de Jonge W J M and Kopinga K 1985 *Phys. Rev.* B **32** 3154
[11] Seitz H and Benner H 1987 *Z. Phys.* B **66** 485
[12] Dashen R F, Hasslacher B and Neveu A 1975 *Phys. Rev.* D **11** 3424
[13] Maki K and Takayama H 1979 *Phys. Rev.* B **20** 3223
[14] Maki K 1981 *Phys. Rev.* B **24** 3991
[15] Mikeska H J 1982 *Phys. Rev.* B **26** 5213
[16] Johnson M D and Wright N F 1985 *Phys. Rev.* B **32** 5798
[17] Riseborough P S 1983 *Solid State Commun.* **48** 901
[18] Giachetti R and Tognetti V 1985 *Phys. Rev. Lett.* **55** 912
[19] Betsuyaku H 1987 *Phys. Rev.* B **36** 799
[20] Mikeska H J and Frahm H 1986 *J. Phys. C: Solid State Phys.* **19** 3203; 1986 *Phys. Rev.* B **34** 3462
[21] Kamieniarz G and Vanderzande C 1987 *Phys. Rev.* B **35** 3341
[22] Currie J F, Trellinger S E, Bishop A R and Krumhansi J A 1977 *Phys. Rev.* B **14** 5567
[23] Mikeska H J 1978 *J. Phys. C: Solid State Phys.* **11** L29
[24] Mikeska H J 1980 *J. Phys. C: Solid State Phys.* **13** 2913
[25] Anderson P W 1952 *Phys. Rev.* **86** 694
[26] Magyari E and Thomas H 1982 *Phys. Rev.* B **25** 531
[27] Jones D H, Pankhurst Q A and Johnson C E 1987 *J. Phys. C: Solid State Phys.* **20** 5149
[28] Jones D H and Chadwick J 1989 *J. Phys. Condens. Mater.* **1** 147
[29] Holyst J A and Sukiennicki A 1988 *Phys. Rev.* B **38** 6975
[30] Etrich C and Mikeska H J 1988 *J. Phys. C: Solid State Phys.* **21** 1582